RSC Advances

Computational Modelling of Tunable Graphene Fresnel lens on Different Substrates

Journal:	*RSC Advances*
Manuscript ID:	RA-ART-05-2014-003991.R1
Article Type:	Paper
Date Submitted by the Author:	09-Jun-2014
Complete List of Authors:	Deng, Sunan; University of Birmingham, School of Mechanical Engineering Jiang, Kyle; University of Birmingham, School of Mechanical Engineering Butt, Haider; University of Birmingham, School of Mechanical Engineering

Journal Name RSCPublishing

ARTICLE

Computational Modelling of Graphene Fresnel lens on Different Substrates

Cite this: DOI: 10.1039/x0xx00000x

Received 00th January 2012,
Accepted 00th January 2012

DOI: 10.1039/x0xx00000x

www.rsc.org/

Sunan Deng, Kyle Jiang and Haider Butt *

Graphene being the thinnest material known has a lot of potential applications in compact systems, where the size and weight are limited. Here we study through computational modelling a graphene based Fresnel zone plate lens. The optical properties of graphene and the focusing response of the lens are studied for the 850 and 1550 nm wavelengths. It is observed that the lens performance can be tuned by adjusting the Fermi level of graphene and the number of layers. The effects of substrates (such as glass and SiO_2/Si) on the performance of graphene lens are also analysed. The result presented can also be used in understanding other graphene based optical devices, such as scattering from graphene based transparent electrodes.

I. Introduction

Fresnel zone plate focuses light by diffracting from a binary mask that blocks part of the radiation.[1] Unlike traditional lenses, Fresnel zone plate has a flat surface with a set of radially symmetric rings, which alternate between opaque and transparent.[2] As Fresnel zone plate offers the possibility of designing high numerical aperture (NA) lens with low weight and small volume, it was widely used in silicon based electronics with various applications, such as optical interconnects,[3] integrated optics,[4] beam focusing[5, 6] and maskless lithography systems.[7]

A thin lens is a lens with a thickness that is negligible compared to the focal length of the lens. Currently, imaging in traditional curved lenses is limited by distortions. Although the aberrations could be corrected by complex optimization techniques, such as aspheric shapes or multilens design, much funding and space will be needed to do so, especially in mid- and near-infrared wavelength range. An alternative is to develop ultrathin lenses with low weight and small volume. Fresnel Zone Plate offers an advanced solution by introducing abrupt changes of optical properties, which breaks our dependence on the propagation effect.

School of Mechanical Engineering, the University of Birmingham, Birmingham B15 2TT, UK
* Email: h.butt@bham.ac.uk, Tel: +44 121 4158623
† Electronic Supplementary Information (ESI) available: Permittivity of 5-layer graphene in Thz (10 μm). See DOI: 10.1039/b000000x/

The ultrathin lens , with a thickness of only 60 nm, which is fabricated by Federico Capasso *et al.*,[8] has attracted enormous attentions as it is considered to be a milestone to revolutionise consumer technology form. As graphene is the thinnest material in the world, we study the properties of graphene Fresnel lens by FDTD method. Graphene, the first 2D material practically realized,[9] is a wonderful optoelectronic material with a set of superior properties, such as high optical transparency, low reflectance and high carrier mobility at room temperature.[10] Accompanying the appealing properties in graphene noted above is its ability of being tunable. The properties of graphene could be changes via changing the charge carriers (electrons or holes), through for example electrical gating[11] or chemical doping.[12] When bias voltage is applied, the optical gap, with the energy proportional to the voltage, will open up. Under realistic conditions, electrical gating can produce chemical potential of $E_F \approx 1$ eV ,[11] which corresponds to additional carriers with concentration[13] of $n \sim 7 \times 10^{13} cm^{-2}$. As photons are uncharged, it is still challenging to control them via electrical means. However, graphene Fresnel lens offers an effective way to manipulate the flow of light energy by changing graphene's Fermi level.

A few papers have been focus on confining light by carbon nanotubes[14-17]. In our previous works[15, 16], we made carbon nanotubes (CNTs) based fresnel lenses, in which CNT arrays act as dark structures because of low reflection, high absorption and random surface scattering. The properties of CNTs (semiconducting or metallic) depend largely on the chiral angle of graphene sheet[18]. However, it's difficult to synthesize large quantities of CNTs with the same chirality. Also CNTs don't have the perfect tunable absorption as graphene, so we propose tunable graphene Fresnel lens here. Beside the tunability, graphene has larger surface area and much thinner than CNTs. So graphene could be used in a complementary way for photonic-nanotube hybrid devices.

Some literature exists on graphene based flat lenses, [19-22] and the focus has been on making plasmonic lenses working in Terahertz range. In some works, people use photonic crystal to focus light and graphene works as a gate to achieve tunability[23, 24]. Compared with their works, we enable both focusing and tunablity function in graphene with two advantages: lower optical losses and greater compactness. Compared with photonic crystal, graphene could have very low optical losses via adjusting its Fermi level to get high carrier density[25].

In Mustafa's work,[26, 27] they proposed tunable THz Fresnel lenses based 2D electron gas at AlGaN/GaN interface and on few-layer graphene sheets. In his study, graphene works as a gate and metal is used as the opaque zones, so the lens is not thin enough due to its multi-layers structure.

In our work, we make graphene to be the opaque zones to explore the thinnest possible lens for compact optical systems. Single layer graphene has a universal optical conductivity[28] of $G_0 = e^2/(4\hbar) \approx 6.08 \times 10^{-5}\Omega^{-1}$, where e is the electronic charge and $\hbar$ is the reduced constant. The transmittance of graphene could be derived by: $T \equiv \left(1+\frac{2\pi G_0}{c}\right)^{-2} \approx 1 - \pi\alpha \approx 0.977$, where $\alpha = \frac{e^2}{4\pi\varepsilon_0\hbar c} = G_0/(\pi\varepsilon_0 c) \approx 1/137$ is the fine structure constant.[29] In the visible regime, the opacity of graphene will increase linearly with the layers of graphene. For N layers graphene, the transmittance could be written as:[30] $T \cong 1 - N\pi\alpha$. So it is possible to use multi-layer graphene as the opaque zone of the Fresnel lenses.

In this paper, the tunable properties of the graphene Fresnel lens under light of wavelength of 850 nm and 1550 nm, which are two important windows in optical communication, are studied by changing the Fermi level of graphene. Our research shows very clear tunable lensing effect of graphene Fresnel lens under the two wavelengths. In comparison to THz, we studied the tenability of graphene Fresnel lens in optical regime, which has potential applications in solar cells, photodiodes, as well as compact optical system, such as cameras and medical imaging systems. Due to the manufacture limit, graphene devices are usually made on different substrates, for example glass and SiO_2/Si. Hence, the interference effect on graphene Fresnel lens caused by different substrates is also discussed.

II. Tunable optical properties of Graphene

In local limit where spatial dispersion effects are negligible, the surface conductivity of graphene can be obtained from the Kubo formula for finite temperatures T, written as:[31]

$$\sigma = \frac{e^2(\omega + i\tau^{-1})}{i\pi\hbar^2}\left[\frac{1}{(\omega+i\tau^{-1})^2}\int_0^\infty \varepsilon\left(\frac{\partial F(\varepsilon)}{\partial\varepsilon} - \frac{\partial F(-\varepsilon)}{\partial\varepsilon}\right)d\varepsilon - \int_0^\infty \frac{F(-\varepsilon)-F(\varepsilon)}{(\omega+i\tau^{-1})^2 - 4\left(\frac{\varepsilon}{\hbar}\right)^2}d\varepsilon\right]$$

$$= \sigma^{intra} + \sigma^{inter} \quad (1)$$

where $F(\varepsilon) = \{1+\exp[(\varepsilon-\mu_c)/K_BT]^{-1}$ is the Fermi Dirac distribution with μ_c the chemical potential; K_B is the Boltzmann constant; $\hbar = h/2\pi$ is the reduced Planck's constant; ω the radian frequency; τ is a phenomenological electron relaxation time, which could be obtained from $\tau = \mu\mu_c/(ev_F^2)$, μ= 10000 cm^2 / (Vs) is the measured dc mobility, e is the electron charge and υ_F= 1 × 10^6 m / s is the Fermi velocity.[32]

In Equation (1) the first term arises from contributions of intraband electron-photon scattering and the second term corresponds to contributions from direct interband electron transitions. When $\mu_c >> K_BT$ (for room temperature, K_BT~26 meV << μ_c), the term for intraband contribution can be simplified as:

$$\sigma^{intra} = \frac{2ie^2K_BT}{\pi\hbar^2(\omega+i\tau^{-1})}\ln\left[2\cosh\left(\frac{\mu_c}{2K_BT}\right)\right] \quad (2a)$$

$$= \frac{ie^2\mu_c}{\pi\hbar^2(\omega+i\tau^{-1})} \quad (\mu_c \gg K_BT) \quad (2b)$$

Similarly the inter band contribution can be simplified as:

$$\sigma^{inter} = \frac{e^2 i(\omega+i\tau^{-1})}{4\pi K_BT} \times \int_0^\infty \frac{G(\xi)}{\frac{\hbar^2(\omega+i\tau^{-1})^2}{(2K_BT)^2} - \xi^2}d\xi \quad (3a)$$

$$= \frac{e^2}{4\hbar}\left[1 + \frac{i}{\pi}\ln\frac{\hbar(\omega+i\tau^{-1}) - 2\mu_c}{\hbar(\omega+i\tau^{-1}) + 2\mu_c}\right] \quad (3b)$$

Eq. (2b) shows that $\boldsymbol{\sigma}^{intra}$ is directly proportional to the chemical potential μ_c, while Eq. (3b) shows that $\boldsymbol{\sigma}^{inter}$ diverges logarithmically when $h\omega \approx 2\ \mu_c$.

In our simulation, the above surface conductivity cannot be directly used. The volume conductivity can be calculated by $\sigma_V = \sigma_S/\Delta$, where Δ= Ntg is the thickness of N-layer graphene and tg=0.34 nm is the monolayer graphene thickness. As graphene is highly anisotropic, only the in-plane component is treated as dispersive. For all our simulation, the graphene is in xz plane and the light emits from the y direction. So the permittivity in different directions could be obtained from the following equations:[33]

$$\varepsilon_{xx} = \varepsilon_{zz} = \varepsilon_r + \frac{i\sigma_v}{\varepsilon_0\omega} = \varepsilon_r + \frac{i\sigma_s}{\varepsilon_0\omega\Delta} \quad (4)$$

$$\varepsilon_{yy} = \varepsilon_r \quad (5)$$

in which $\boldsymbol{\varepsilon}_0$ is the vacuum permittivity and the dielectric permittivity can be introduced as $\varepsilon_r = 2.5$.[34] In this paper, all the permittivity we discuss is the permittivity of x direction.

We studied the permittivity of 5-layer and 10-layer graphene under the 850 nm and 1550 nm wavelengths. Figure 1 demonstrates the contributions of intraband and interband on permittivity of 5-layer graphene when illuminated with 850 nm and 1550 nm wavelengths. In Figure 1, the red lines represent for graphene permittivity with 850 nm incident light, while the black ones represent for permittivity with 1550 nm light; the dotted lines are contributions raised from intraband and the dash lines are contributions due to interband, while the solid lines considers both the contribution of interband and intraband. Figure 1(a) illustrates that in the calculation of the real permittivity of graphene under light of 850 nm and 1550 nm, contributions of both intraband and interband should be considered. The peaks of real permittivity are contributed by intraband, while the contributions of interband are linear. Compared with the peak of graphene real permittivity under 850 nm, the peak of 1550 nm is higher and left shifted. Moreover, the real permittivity of 1550 nm is dominated by intraband at high Fermi level (above the peak value of 0.4 eV). From S1 in Appendix, it can be observed that for larger wavelength (10 µm), the peak of graphene real permittivity will shift towards low Fermi level and the permittivity will be dominated by intraband. Figure 1(b) shows that the graphene imaginary permittivity is dominated by interband, and the contributions of intraband could be neglected. At the peak positions of graphene real permittivity (0.73 eV for 850 nm, 0.4 eV for 1550 nm), there are sharp edges in imaginary permittivity. At lower Fermi energies (smaller than 0.4eV), the graphene imaginary permittivity for 1550 nm is higher than 850 nm.

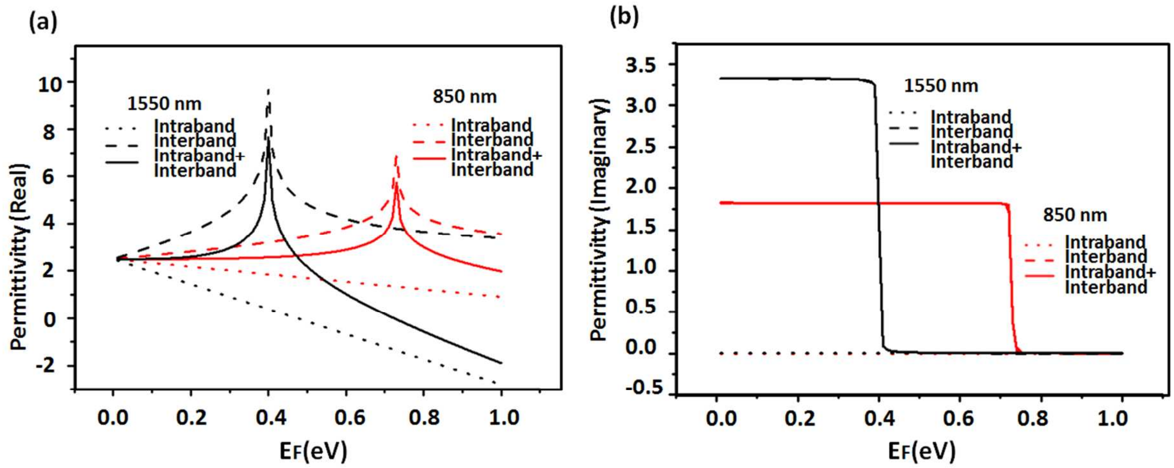

Figure1. Permittivity of 5-layer graphene for 850 nm and 1550 nm wavelengths with respect to the Fermi level. (a) Real permittivity of graphene considers contributions of intraband (the dotted lines), interband (the dash lines), both intraband and interband (solid lines) (b) Imaginary permittivity of graphene considers contributions of intraband (the dotted lines), interband (the dash lines), both intraband and interband (solid lines)

We have also studied the permittivity of 10-layer graphene at 850 nm and 1550 nm wavelengths with respect to Fermi energies. As shown in Figure 2(a), when shine with the same light, the peaks of graphene real permittivity are at the same positions and the peaks for 10-layer graphene are lower than 5-layer graphene. Figure 2(b) demonstrates that the imaginary permittivity of graphene with the same light has the same sharp edges. Before the sharp edges, the imaginary permittivity of 5-layer graphene is higher than 10-layer graphene

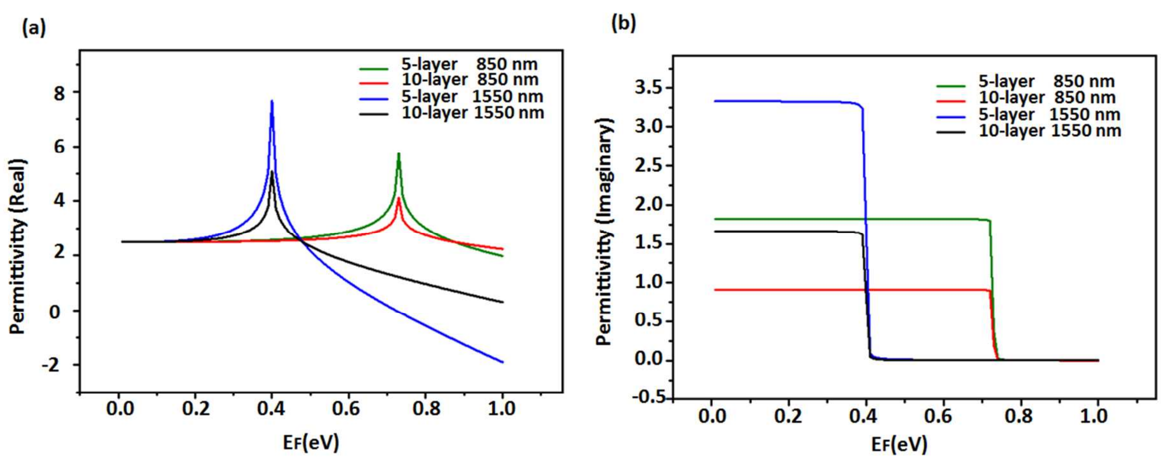

Figure 2. **Permittivity of 5-layer and 10-layer graphene under light of 1550 nm and 850 nm.** (a) Real permittivity of 5-layer and 10-layer graphene (b) Imaginary permittivity of 5-layer and 10-layer graphene.

III. Graphene based Ultra-thin Fresnel lenses

The graphene Fresnel zone plate was designed according to the equation[35]: $\frac{f}{R_n} = \frac{R_n}{n\lambda}$ (where λ is the wavelength of light, n=1, 2, 3…), and the radius of the *n*th zone (R_n) in a Fresnel lens $R_n^2 = nR_1^2$ (for n>1). In our simulation R_1=10 μm, n_{max}=23, so the diameter of the lens is about 94 μm.

Due to the circular symmetry of the Fresnel zone plates, 2D simulations were performed. The graphene lens was placed on the X plane and the light is from Y direction. Figure 3(a) shows the computed power flow distribution of the light reflected by the Fresnel lens. The lens was made from 5-layer graphene at Fermi level 0.73eV, illuminated with 850 nm wavelength light. The horizontal and vertical cross sectional lines at the focal point are shown in Figure 3(b) and (c) (red lines), respectively. The simulation confirms the focusing of the reflected light of the graphene-based Fresnel lens. Figure 3(b) and (c) also show the influence of varying Fermi levels on the lensing effect, while Figure 3(d) and (e) illustrate the influence of the thickness of graphene on lensing effect.

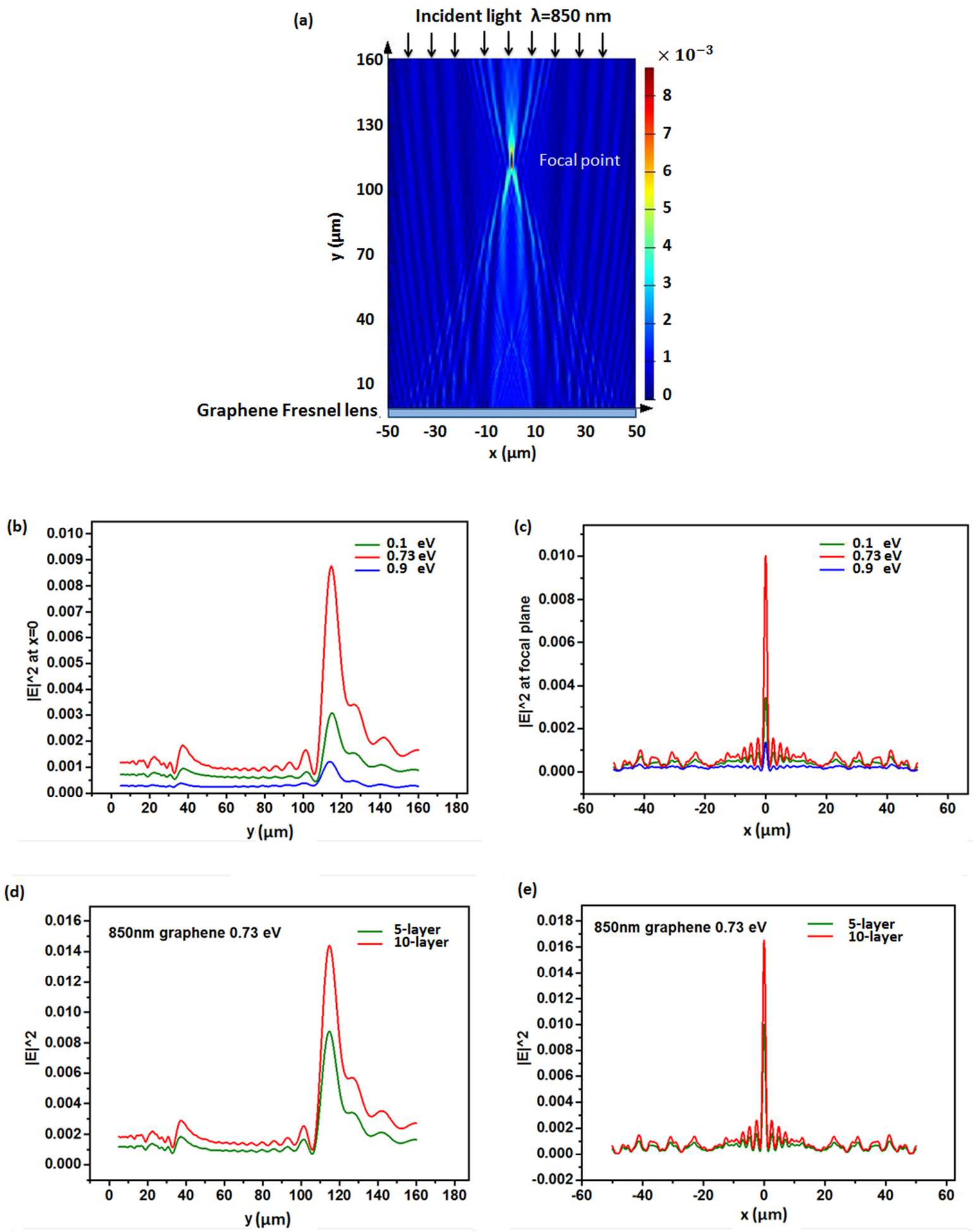

Figure 3. Graphene Fresnel lens illuminated by light of 850 nm (a) Power flow distribution of light reflected from the 5-layer graphene Fresnel lens when illuminated by 850 nm light (Fermi level 0.73 eV). The lens is located at y=0. (b) Power flow distribution across the y-axis, extracted at x=0. (c) Power flow distribution across the x-axis, at the focal plane. In (b) and (c), the green, red and blue lines correspond with graphene Fermi levels of 0.1 eV, 0.73 eV and 0.9 eV respectively. Power flow distribution across (d) y-axis and (e) x-axis for 5-layer (green line) and 10-layer (red line) graphene lens.

In Figure 3(b) and (c), the green lines and blue lines are intensity distribution of cross section lines at focal point when the Fermi level of graphene is 0.1 eV and 0.9 eV, respectively. The focal point power intensity of graphene Fresnel lens with 0.73 eV Fermi level is almost three times as high as that at Fermi level 0.1 eV and nine times as high as that at Fermi level 0.9 eV. This phenomenon is caused by different permittivity of graphene with different Fermi levels, as shown in Figure 1(a). The focal point intensity of graphene Fresnel lens with 0.73 eV Fermi level is much higher due to the high real permittivity (peak) and low imaginary permittivity(almost 0). The focal point intensity of 0.1 eV is higher than 0.9 eV because of higher real and imaginary permittivities. The results show that the focal point intensity can be adjusted by changing graphene's Fermi level which in turn changes the optical properties (dielectric constant and absorption) of the Fresnel zones. The performance of the lens is improved with an increase contrast in the difference of optical properties between the transparent (air) and opaque zones (graphene). As shown in Figure 3(d) and (e), the power intensity at the focal point increases for nearly two times when the layer number increases from 5 to 10, owing to the increased light reflection.

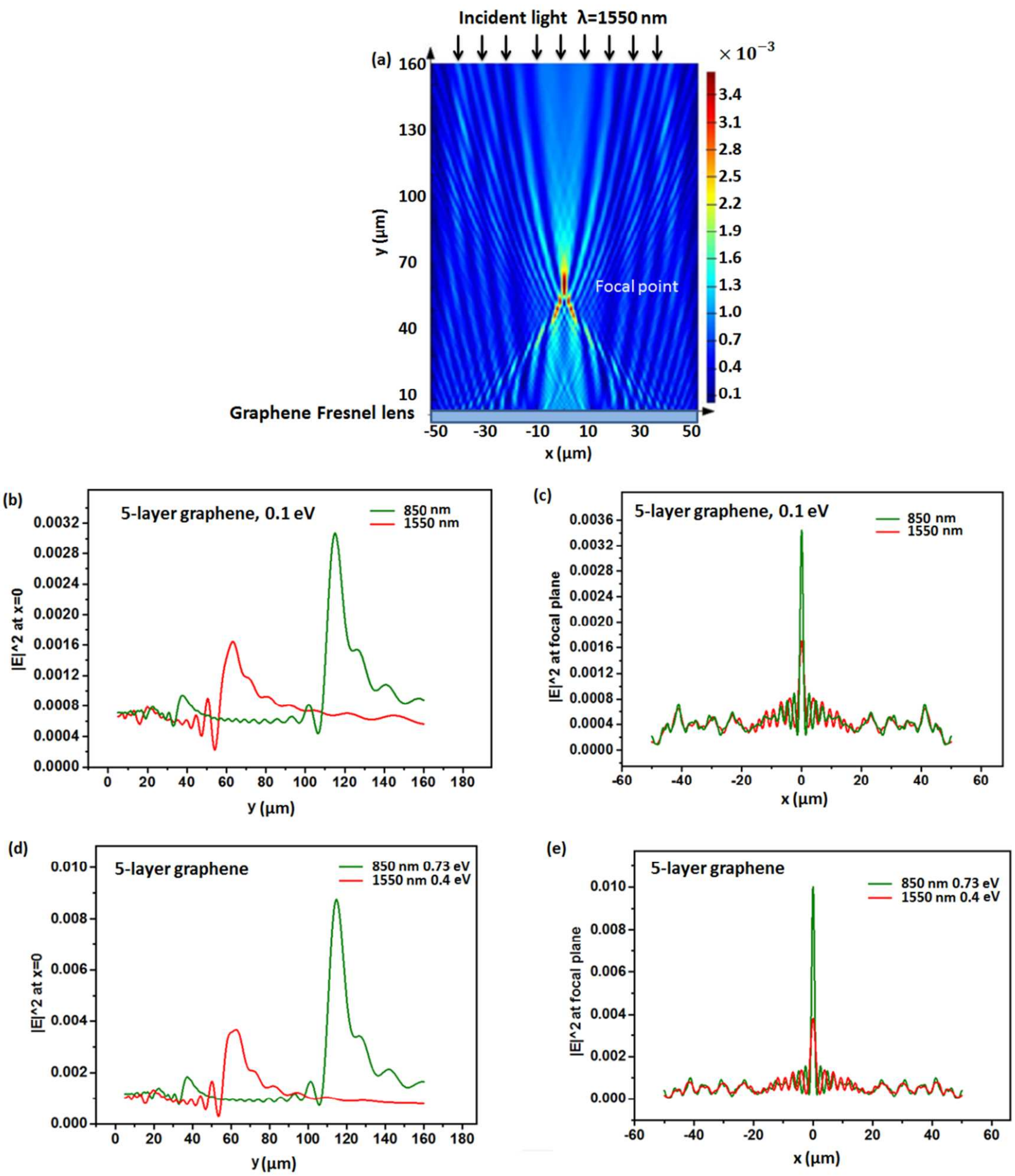

Figure 4. (a) Power flow reflected from 5-layer graphene Fresnel lens when illuminated with light of 1550 nm (Fermi level 0.4 eV), (b) Power flow distribution along x=0, (c) Power flow distribution at the focal plane, (d) Power flow distribution along x=0 and (e) the focal plane for lens illuminated by of 850 nm (with Fermi level at peak real permittivity: 0.73 eV) and 1550 nm (with Fermi level at peak real permittivity: 0.4 eV).

Next we studied the influence of different wavelengths on the lensing effect. Figure 4(a) is the power flow intensity distribution of the reflected light by 5-layer graphene Fresnel lens (Fermi level is the peak value 0.4 eV), illuminated by 1550 nm light. Compared with Figure 3(a), the focal length in Figure 4(a) changes from 115 μm (theoretical value for 850 nm is 117.65 μm) to 63.25 μm (theoretical value for 1550 nm should be 64.51 μm). Figure 4(b) and (c) shows the horizontal and vertical cross sectional lines at the focal point both for 850 nm and 1550 nm light with the same Fermi level (0.1 eV). The focal point intensity of 1550 nm is much lower than 850 nm, which means that the graphene Fresnel lens with Fermi level 0.1 eV has better lensing effect at 850 nm. This may due to that the imaginary permittivity of graphene (Fermi level 0.1 eV) under 1550 nm light is nearly twice of that under 850 nm light while graphene's real permittivities under both wavelengths are almost same. A higher imaginary permittivity causes losses leading to reduced reflection.

Figures 4(d) and 4(e) compares the focal intensity distribution when the graphene Fresnel lens is illuminated with light of 850 nm and 1550 nm with Fermi levels of peak real permittivities (for 850 nm is 0.73 eV, for 1550 nm is 0.4 eV). The focal point intensity of 1550 nm is still much lower than 850 nm light. The possible reason again could be more absorption related losses due to a higher imaginary permittivity.

IV. Influence of different substrates

The graphene devices are usually made on various substrates, such as glass and SiO_2/Si. Hence we simulate graphene Fresnel lens on these substrates.

According to Skulason *et al,*[36] few-layer graphene on glass could have very high reflection contrast, where the reflection contrast could be written as: $C_R = \frac{R_g - R_0}{R_0}$, with R_g is reflectance of air-graphene-glass, and R_0 is reflectance of the air-glass interface. This indicates the possibility of making Fresnel lenses on glass.

Figure 5(a) illustrates the power flow of the reflection of 5-layer graphene Fresnel lens (Fermi level 0.1 eV) on 5 μm thick glass substrate, illuminated with light of 850 nm wavelength. Clearly focal point could be seen from Figure 5(a), but not as clear as Figure 3(a). The figure consists of an interference pattern produced by the glass substrate.

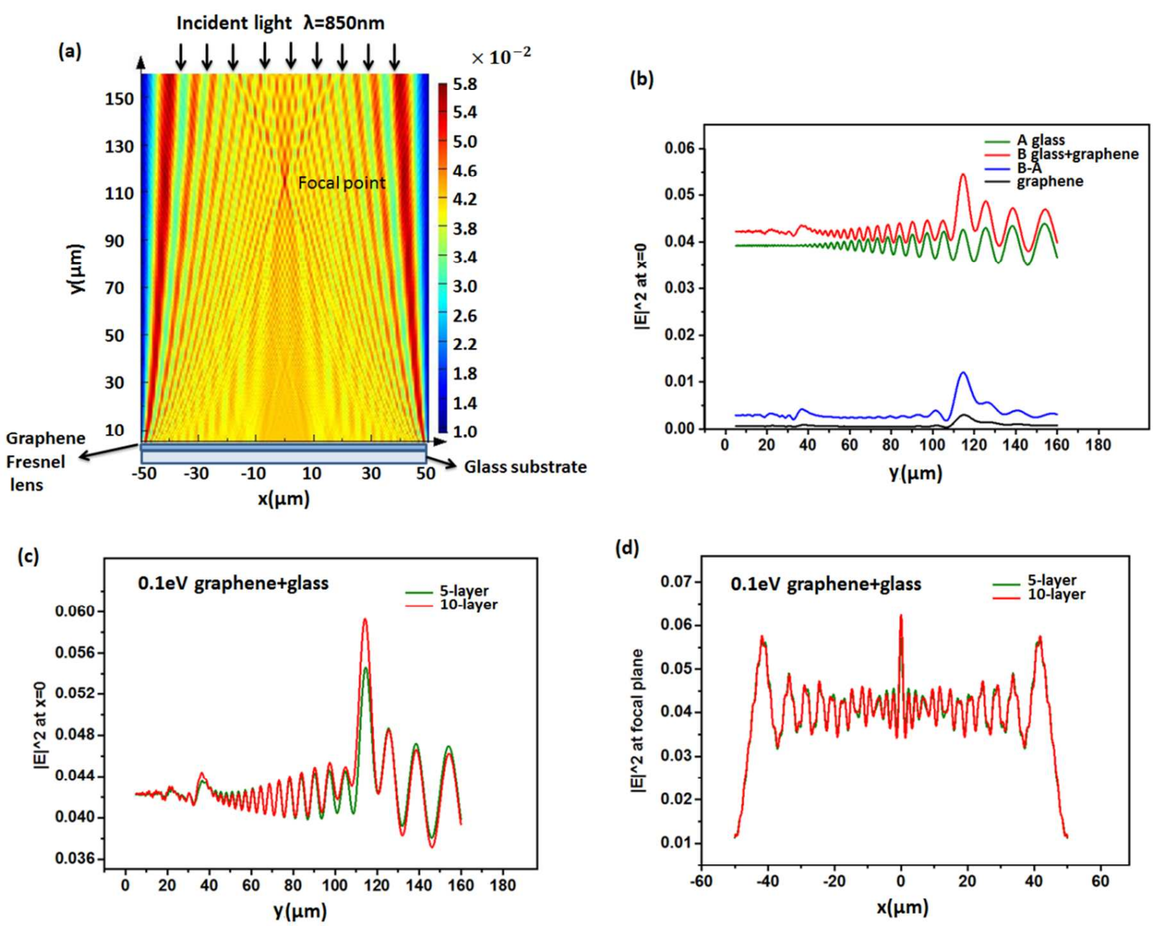

Figure 5. Graphene Fresnel lens on glass substrate. (a) Power flow reflected from 5-layer graphene Fresnel lens on glass substrate when illuminated by light of 850 nm(Fermi level 0.1 eV) (b) Power flow across y-axis, extracted from x=0. The green line, red line and black line correspond with power flow when light is shined on glass substrate, graphene lens on glass substrate, and on a graphene lens respectively. The blue line is the result of the green line subtracted from the red line. The power flow distribution in across (c) y (at x=0) and (d) x-axis (at focal point) for 5-layer and 10-layered graphene lens.

Figure 5(b) compares the intensity distribution along the cross sectional lines at the focal point of graphene Fresnel lens with and without glass substrate. In this Figure, the black line shows the intensity distribution of the graphene lens without the substrate, red line shows the distribution for the graphene lens with a glass substrate, and the green line shows the distribution light is shined only on the 5 μm thick glass substrate.

Compared with the black line (graphene Fresnel lens without substrate), it could be seen that the wave shape of the red line consists of an interference effect produced by the glass substrate. When the influence of glass is subtracted from the red line we observe a clear focusing effect shown as B-A (blue line) in the figure.

The study of different layered graphene Fresnel lens in Figure 5(c) and (d) also shows that the interference wave is caused by glass substrate while the focal lensing effect is caused by graphene. Figure 5(c) and (d) demonstrate that 5-layer and 10-layer graphene Fresnel lenses on glass have almost the same interference wave, but 10-layer graphene Fresnel lens will make more contribution to the focal lensing effect, due to the increasing reflection.

The interference effect of the substrates can be explained by the interference theory of light, which is related to the wavelength of incident light as well as the thickness of the substrate. To get the optimized lensing effect, we explore the relationship between the thickness of glass substrate and the reflection of the 5-layer graphene lens/glass structure, with graphene Fermi level 0.73 eV. Figure 6 (a) shows the effective reflection from the graphene Fresnel lens/glass changes when we change the thickness of the glass substrates from 4.3 μm to 5 μm, and the step is 50 nm. In our simulation, the monitor was put on 1 μm above the graphene lens, and the reflection is the total reflected power flow passing the monitor. Periodic change of reflection could be seen from Figure 6(a), and the period is 300 nm. Theoretically, if there is only a glass substrate, the period should be $\lambda/2$=425 nm. The difference between the simulation value and the theoretic value may due to the effect of the 5 layer-graphene Fresnel lens. As can be seen, the shape of the reflection curve is not smooth enough, and this may be caused by the large sweep step.

We also choose different thicknesses of substrates to calculate the power distribution along the vertical line across the focal plane, as shown in Figure 6(b). The green line represents the power distribution of the 4.75 μm thick substrate shown as A in Figure 6(a). This graph represents the peak reflection caused by the cavity. The red line in Figure 6(b) is the power distribution with glass substrate thickness at point B (4.9 μm), which has the lowest reflection.

In addition it is reported that graphene has a high optical contrast on the substrate of SiO_2/Si, especially when the thickness of SiO_2 is 300 nm. [37, 38] The performance of the graphene Fresnel lens was studied on SiO_2/Si substrate. Figure 7(a) shows the power intensity of reflection from 5-layer graphene Fresnel lens (Fermi level 0.1 eV) on substrate of SiO_2/Si substrate, which is consisted of a 300 nm SiO_2 layer and 5 μm Si. Lensing effect can hardly be observed due to the strong interference produced by the substrate. In Figure 7(b), the power distributions across y-axis are shown for silicon substrate (black line) and silicon substrate with a graphene lens (blue line). The comparison of the two curves shows the light focusing effect produced by the graphene lens. SiO_2/Si substrate due to the thin film of SiO_2 produces a stronger cavity interference response compared to the glass substrate.

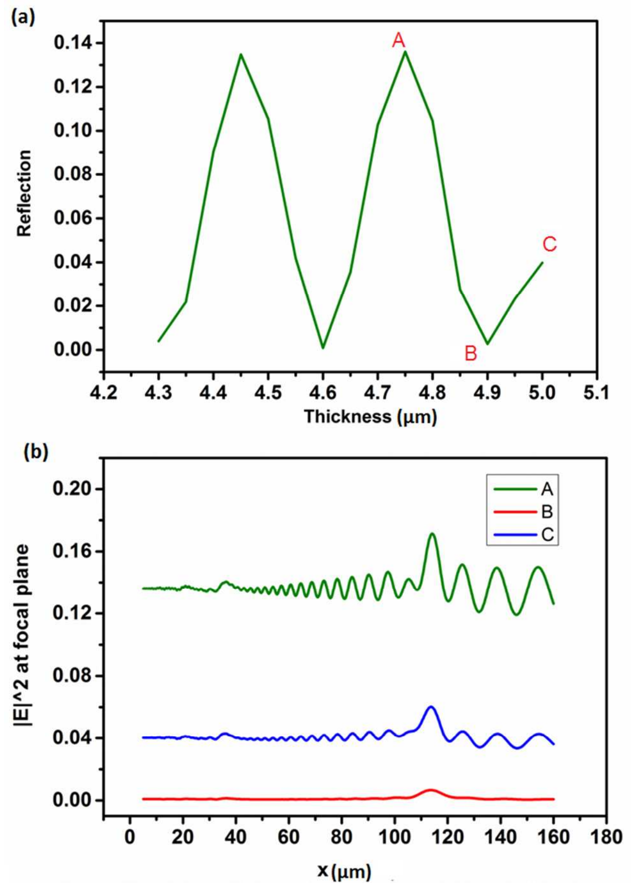

Figure 6. (a) The reflection of 5-layer graphene Fresnel lens on glass substrate with the changing substrate thickness. (b) Power flow distribution along the vertical line across the focal plane. The green, blue and red line represents the power distribution when the substrate thickness equal to points A, B, and C in (a), respectively.

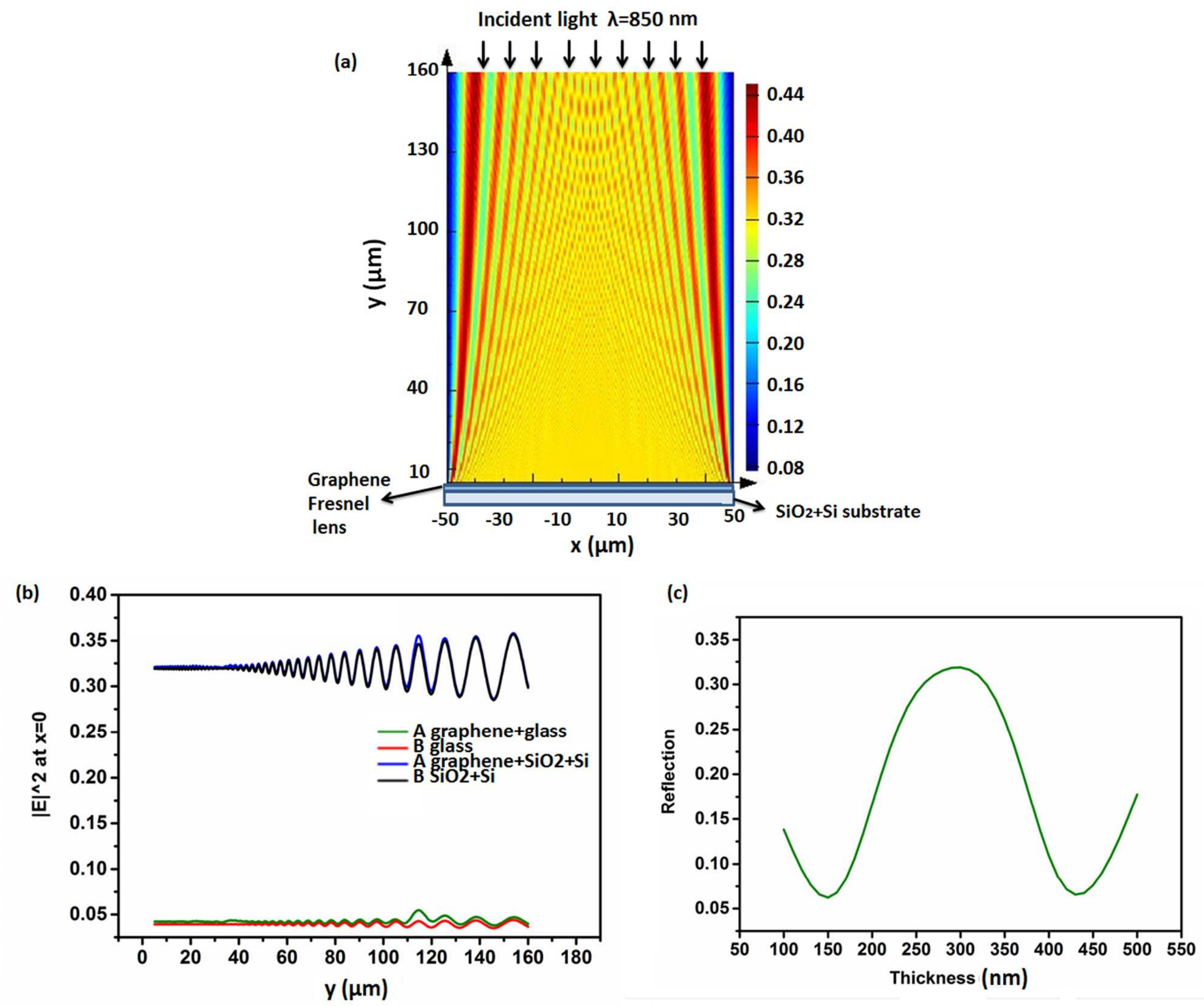

Figure 7. 5-layer graphene Fresnel lens (Fermi level 0.1 eV) on SiO_2/Si substrate. (a) Power flow reflected from 5-layer graphene Fresnel lens on SiO_2/Si substrate (consisting of 300 nm SiO_2 layer and 5 μm silicon). (b) Power flow across the y-axis at x=0. The red and green lines represent the power flow when 850 nm light illuminates a glass substrate and a 5-layer graphene Fresnel lens on glass substrate. The black and blue lines show the power flow when light is projected on a SiO_2/Si substrate and a 5-layer graphene lens on SiO_2/Si substrate. (c) The reflection of the 5 layer-graphene Fresnel lens on SiO_2/Si changes with the thickness of SiO_2.

The graphene/SiO_2/Si structure could be seen as a sort of Fabry-Perot cavity,[39] with graphene playing a role of the input/output barriers and SiO_2 the spacer. According to the principle of Fabry-Perot cavity, the optical contrast of graphene could be adjusted by changing the thickness of spacer or the wavelength of light. We change the thickness of SiO_2 from 100 nm to 500 nm, with a step of 10 nm, and the change of reflection can be seen from Figure 7(c). When the thickness of SiO_2 is 300 nm, the graphene/SiO_2/Si structure has peak reflection. However, the reflection is very low when the thickness is 150 nm and 440nm. So if we change the thickness of SiO_2 from a larger range, we can see the reflection changes periodically and the period is about 300 nm, which is consistent with the results in Figure 6(a).

V. Conclusions

In summary, we have explored the tunable properties of graphene Fresnel lens under illumination of 850 nm and 1550 nm, which are two important wavelengths for optical communication. By adjusting the Fermi level of graphene, the intensity of focal point changes. The properties of graphene on glass and SiO_2/Si substrates are also studied. When the incident light is fixed, the thickness of substrates plays an important role in producing the interference patterns which affect the focusing ability of the lenses. The results presented can also be used to explain the properties of other graphene based optical devices using similar substrates.

Acknowledgements

The authors thank The Leverhulme Trust for the research funding.

Supporting Information

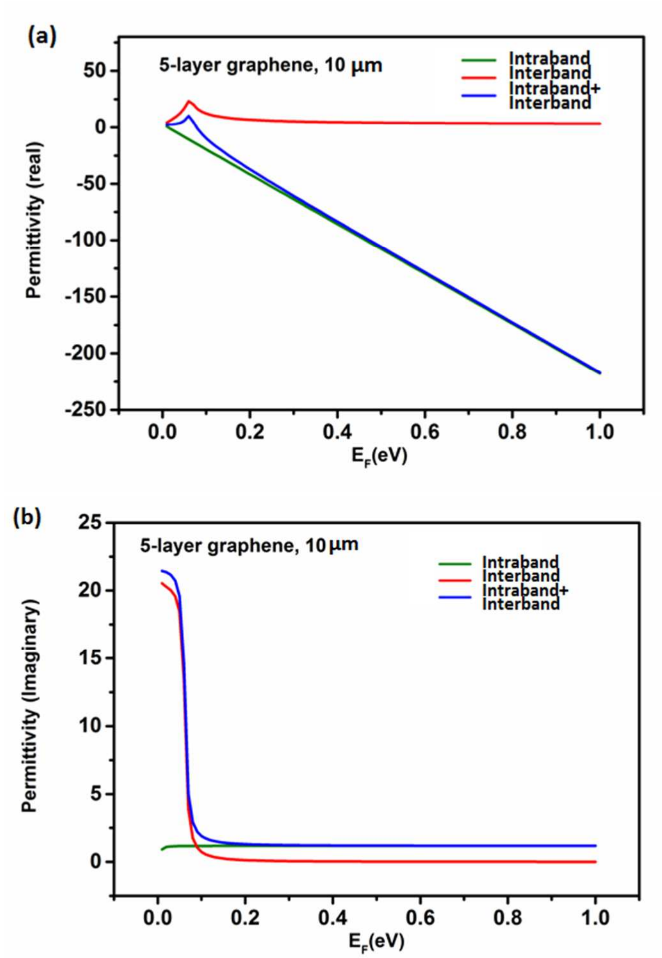

Figure S1: The properties of 5-layer graphene in THz (10 μm)

When the Fermi level is bigger than 0.1 eV, the influence of interband could be neglected, and the relationship between real permittivity and Fermi Level is linear.

References

1. Aničin, B.; Babović, V.; Davidović, D. American Journal of Physics 1989, 57, 312.

2. Rastani, K.; Marrakchi, A.; Habiby, S. F.; Hubbard, W. M.; Gilchrist, H.; Nahory, R. E. Applied Optics 1991, 30, (11), 1347-1354.

3. Ferstl, M.; Frisch, A.-M. Journal of Modern Optics 1996, 43, (7), 1451-1462.

4. Kodate, K.; Tokunaga, E.; Tatuno, Y.; Chen, J.; Kamiya, T. Applied Optics 1990, 29, (34), 5115-5119.

5. Fallahi, M.; Kasunic, K. J.; Penner, S.; Nordman, O.; Peyghambarian, N. OPTICE 1998, 37, (4), 1169-1174.

6. Morgan, B.; Waits, C. M.; Krizmanic, J.; Ghodssi, R. Microelectromechanical Systems, Journal of 2004, 13, (1), 113-120.

7. Carter, D. J. D.; Gil, D.; Menon, R.; Mondol, M. K.; Smith, H. I.; Anderson, E. H. Journal of Vacuum Science & Technology B 1999, 17, (6), 3449-3452.

8. Aieta, F.; Genevet, P.; Kats, M. A.; Yu, N.; Blanchard, R.; Gaburro, Z.; Capasso, F. Nano Lett 2012, 12, (9), 4932-4936.

9. Novoselov, K. S.; Geim, A. K.; Morozov, S.; Jiang, D.; Zhang, Y.; Dubonos, S.; Grigorieva, I.; Firsov, A. science 2004, 306, (5696), 666-669.

10. Butt, H.; Kidambi, P. R.; Dlubak, B.; Montelongo, Y.; Palani, A.; Amaratunga, G. A.; Hofmann, S.; Wilkinson, T. D. Advanced Optical Materials 2013, 1, (11), 869-874.

11. Chen, C.-F.; Park, C.-H.; Boudouris, B. W.; Horng, J.; Geng, B.; Girit, C.; Zettl, A.; Crommie, M. F.; Segalman, R. A.; Louie, S. G. Nature 2011, 471, (7340), 617-620.

12. Liu, H.; Liu, Y.; Zhu, D. Journal of Materials Chemistry 2011, 21, (10), 3335-3345.

13. García de Abajo, F. J. ACS Photonics 2014.

14. Nikolaenko, A. E.; Papasimakis, N.; Chipouline, A.; De Angelis, F.; Di Fabrizio, E.; Zheludev, N. I. Opt. Express 2012, 20, (6), 6068-6079.

15. Rajasekharan, R.; Butt, H.; Dai, Q.; Wilkinson, T. D.; Amaratunga, G. A. Advanced Materials 2012, 24, (23), OP170-OP173.

16. Butt, H.; Rajesekharan, R.; Dai, Q.; Sarfraz, S.; Vasant Kumar, R.; Amaratunga, G. A. J.; Wilkinson, T. D. Applied Physics Letters 2012, 101, (24), -.

17. Zhang, Q.; Hároz, E. H.; Jin, Z.; Ren, L.; Wang, X.; Arvidson, R. S.; Lüttge, A.; Kono, J. Nano Lett 2013, 13, (12), 5991-5996.

18. Baughman, R. H.; Zakhidov, A. A.; de Heer, W. A. Science 2002, 297, (5582), 787-792.

19. Andryieuski, A.; Lavrinenko, A. V.; Chigrin, D. N. Physical Review B 2012, 86, (12), 121108.

20. Wang, G.; Liu, X.; Lu, H.; Zeng, C. Scientific reports 2014, 4.

21. Tamagnone, M.; Gomez-Diaz, J.; Mosig, J. R.; Perruisseau-Carrier, J. Applied Physics Letters 2012, 101, (21), 214102.

22. Forati, E.; Hanson, G. W.; Yakovlev, A. B.; Alù, A. arXiv preprint arXiv:1311.4791 2013.

23. Majumdar, A.; Kim, J.; Vuckovic, J.; Wang, F. Nano Lett 2013, 13, (2), 515-518.

24. Gan, X.; Shiue, R.-J.; Gao, Y.; Mak, K. F.; Yao, X.; Li, L.; Szep, A.; Walker Jr, D.; Hone, J.; Heinz, T. F. Nano Lett 2013, 13, (2), 691-696.

25. Bao, Q.; Loh, K. P. ACS nano 2012, 6, (5), 3677-3694.

26. Karabiyik, M.; Al-Amin, C.; Das, S.; Pala, N.; Choi, W. B. In Subwavelength, multimode, tunable plasmonic terahertz lenses and detectors, SPIE Defense, Security, and Sensing, 2012; International Society for Optics and Photonics: pp 83630L-83630L-8.

27. Karabiyik, M.; Al-Amin, C.; Pala, N. Terahertz Science and Technology, IEEE Transactions on 2013, 3, (5), 1-8.

28. Kuzmenko, A.; Van Heumen, E.; Carbone, F.; Van Der Marel, D. Physical review letters 2008, 100, (11), 117401.

29. Nair, R.; Blake, P.; Grigorenko, A.; Novoselov, K.; Booth, T.; Stauber, T.; Peres, N.; Geim, A. Science 2008, 320, (5881), 1308-1308.

30. Bonaccorso, F.; Sun, Z.; Hasan, T.; Ferrari, A. Nature Photonics 2010, 4, (9), 611-622.

31. Gan, C. H.; Chu, H. S.; Li, E. P. Physical Review B 2012, 85, (12), 125431.

32. Grigorenko, A.; Polini, M.; Novoselov, K. Nature photonics 2012, 6, (11), 749-758.

33. Vakil, A.; Engheta, N. Science 2011, 332, (6035), 1291-1294.

34. Falkovsky, L. In Optical properties of graphene, Journal of Physics: Conference Series, 2008; IOP Publishing: p 012004.

35. Fan, Y.-H.; Ren, H.; Wu, S.-T. Opt. Express 2003, 11, (23), 3080-3086.

36. Skulason, H.; Gaskell, P.; Szkopek, T. Nanotechnology 2010, 21, (29), 295709.

37. Casiraghi, C.; Hartschuh, A.; Lidorikis, E.; Qian, H.; Harutyunyan, H.; Gokus, T.; Novoselov, K.; Ferrari, A. Nano Lett 2007, 7, (9), 2711-2717.

38. Blake, P.; Hill, E.; Castro Neto, A.; Novoselov, K.; Jiang, D.; Yang, R.; Booth, T.; Geim, A. Applied Physics Letters 2007, 91, (6), 063124-063124-3.

39. Roddaro, S.; Pingue, P.; Piazza, V.; Pellegrini, V.; Beltram, F. Nano Lett 2007, 7, (9), 2707-2710.

Journal Name RSCPublishing

ARTICLE

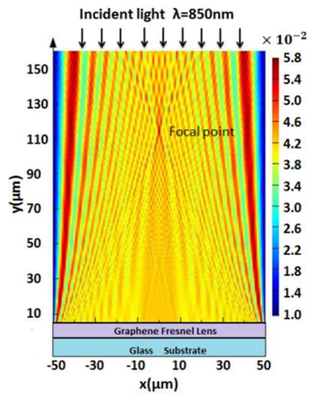

Size: 5.26cm×4cm

Highlight: In this work we studied tuanble lensing effects of graphene Fresnel lens on different substrates with incident light of 850nm and 1550nm waelengths.